IDENTIFICATION AND ASSESSMENT OF A NONLINEAR DYNAMIC ACTUATOR MODEL FOR GUST LOAD ALLEVIATION IN A WIND TUNNEL EXPERIMENT

M. Tang, M. Böswald, Y. Govers
German Aerospace Center (DLR), Institute of Aeroelasticity
Goettingen, D-37073
Germany

M. Pusch
German Aerospace Center (DLR), Institute of System Dynamics and Control
Oberpfaffenhofen-Wessling, D-82234
Germany

Overview

The actuator dynamics of an active load alleviation system for a low speed wind tunnel model is investigated. For the design of the control law a model, consisting of aerodynamics, structural dynamics and actuator dynamics is required. While methods for modeling of aerodynamics and structural dynamics exist, an equivalent model for the actuator must be determined experimentally. A nonlinear actuator model is derived and its parameters are identified. The impact of nonlinearities on the control performance is quantified in simulations.

1 INTRODUCTION

Within the internal research activity “KonTeKst” [1-3] of the German Aerospace Center (DLR), the benefits of an active load alleviation system has been investigated. The test object is a flexible wing of 1.5m span with three trailing edge control surfaces, each one actuated by a dedicated servo. The wing root is mounted on a pitch excitation system used to simulate gust encounter for exciting the wing. The test campaign was performed in the Cross-wind Simulation Facility (Seitenwindkanal Goettingen, SWG), which is a low speed closed circuit wind tunnel operated at ambient static pressure and ambient temperature, see Figure 1. For the design of the control law a numerical model of the open-loop system, consisting of the aerodynamics, the structural dynamics, and the actuator dynamics is required.

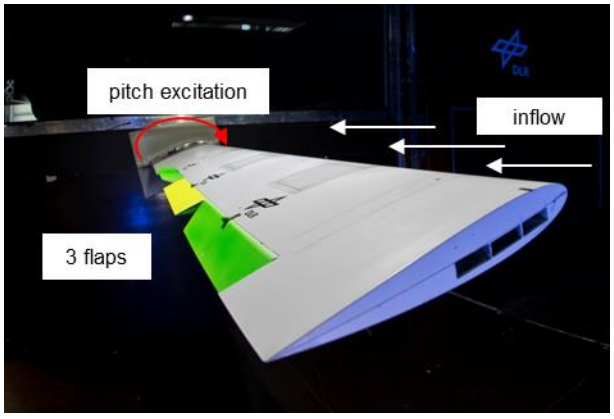

Figure 1 Wind tunnel model with pitch excitation and three trailing edge control surfaces

Fung [4] proposed a block diagram to visualize the relation between the elastic, inertia and aerodynamic forces, as can be seen in Figure 2. The load alleviation system adds the control law (blue) and the actuator model (red), which will affect the global system behavior. While numerical methods for the mathematical modeling of aerodynamics and structural dynamics exist, an equivalent model for the actuator dynamics must be determined experimentally. Static properties of servos are given by the manufacturer but the overall dynamics can only be estimated after physical assembly of all subsystems. It is well known that actuators also show nonlinear behavior. Typical nonlinearities are free play, rate limit and power limit. For control law design and gust response analysis however, these nonlinearities are commonly neglected and instead a linearized model is used. In order to show the differences to the nonlinear model, the impact of the mentioned nonlinearities on control performance is studied.

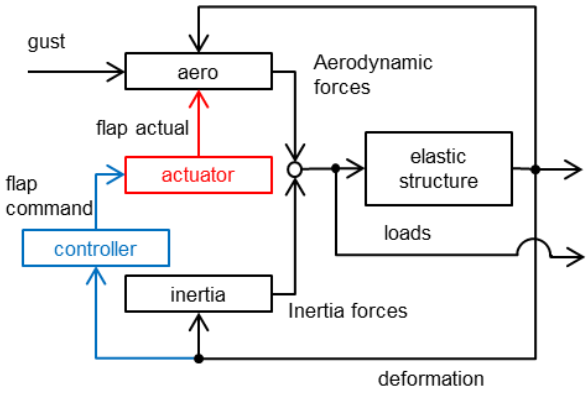

Figure 2 Block diagram of aeroservoelastic systems

The goal of the implemented gust load alleviation system is to reduce the wing root bending moment by a coordinated deflection of the three trailing edge flaps based on eight vertical acceleration measurements. The according control law is designed using the approach described by Pusch et. al [5], which suggests an $\mathcal{H}_2$-optimal blending of control inputs and measurement outputs. In doing so, the loads-dominating aeroelastic modes can be effectively isolated and subsequently damped by a simple single-input single-output (SISO) controller. The resulting closed-loop interconnection is depicted in Figure 3. The controller performance greatly depends on the performance of the actuation system driving the flaps, which is often limited by nonlinearities like saturation or free play as investigated herein.

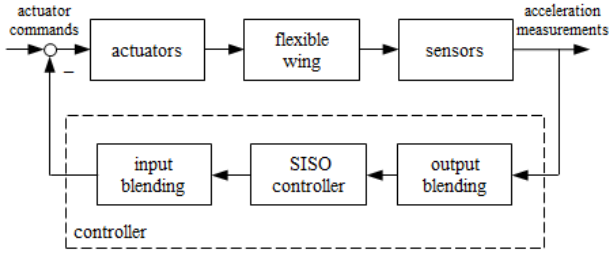

Figure 3 Closed-loop Interconection

Nonlinearities have been extensively studied for hydraulic actuators of full scale aircraft. Taylor et. al [6] assessed the impact of nonlinear actuator dynamics on flight control performance. Fielding and Flux [7] give an overview of common nonlinearities in hydraulic systems and analyze them with appropriate methods. Also the modelling of hydraulic actuators is described in their work. Stirling and Cowling [8] modelled a hydraulic actuator for a combat aircraft and simulated the nonlinear behavior of the actuation system. Banavara and Newsom [9] studied the effect of a nonlinear actuator in a full scale aircraft. Therein, the open- and closed-loop system behavior is studied in time domain using a linear model of the aerodynamics and structural dynamics and adding a nonlinear actuator model.

However in the “KonTeKst” project, the test object is rather small so that electric servos have been chosen as driving elements of the actuator providing better performance within little available space. Nevertheless the nonlinearities given in the literature for hydraulic actuators are generic, so that those are also applicable for electric servo motors. Also the theoretical methods used to study and simulate the actuation systems can be adapted for this application. Furthermore, the objective here is to reduce structural loads, which in contrast to flight control typically requires a higher actuator bandwidth.. Regan [10] tested several electric servo motors in an extensive study for active flutter suppression. Therein, amplitude dependent system behavior was detected, which indicates a nonlinear system behavior. For controller design linear actuator dynamics are commonly assumed while possibly occurring nonlinearities are considered by enforcing sufficiently high robustness margins, see e.g. Theis et. al [11] or Pusch et. al [12]

In the literature hydraulic actuators for real aircraft have been primarily assessed for flight control laws whereas the interest for this experiment lies in electric servo motors for active loads alleviation. Typically, an interaction between structural modes and actuators are not desired in flight control. However, it is a prerequisite for this experiment that the actuator can effectively change the properties of the structural modes. Hence, the research on nonlinear hydraulic actuator is adapted for this experiment in order to assess the effect on the performance of the active load alleviation. First typical nonlinearities in actuators are described. In the subsequent section the design of the implemented actuation system is shown. Then the impact of existing nonlinearities on controller performance is assessed in simulations. Finally, the parameters for the nonlinear actuator model are identified.

2 NONLINEARITIES IN ACTUATION SYSTEMS

Typical nonlinearities for actuators are deflection-, rate- and acceleration limitations as well as free play in the mechanical integration. The maximum deflection is given by the geometry of the flap and the actuation system. Often software limits are employed such that the flap stops before running into physical limitations. The servo motor itself allows a maximum velocity or rate limit and a maximum acceleration since the maximum torque is also limited. Furthermore, internal electronics introduces dead time, especially by digital signal processing, since the command signals are generated each time step and remains constant in between. The processor must wait a certain time, until the data is processed. Additionally the mechanics introduce free play.

Nonlinear behavior leads to far more complicated numerical simulations. Therefore describing functions are used to simplify the analysis, as discussed by Fielding and Flux [7]. If a linear system is excited by a single sine signal, it will respond with a sine signal at the excitation frequency. In contrast, nonlinear systems respond with integer multiples of the fundamental sine excitation and the response is amplitude dependent. In the describing function analysis, the response is reduced to the fundamental harmonic, as shown in equation (1).

$$a = \int_0^T y e^{j\omega t} dt, \tag{1}$$

where a is the complex response reduced to the fundamental frequency, ω is the frequency of excitation, and y is the response of the system. Repeating this analysis for different excitation amplitudes allows then describing the amplitude dependent behavior. This analysis is used here to describe the amplitude gain and phase shift of chosen nonlinearities on the response for single stationary sine excitation.

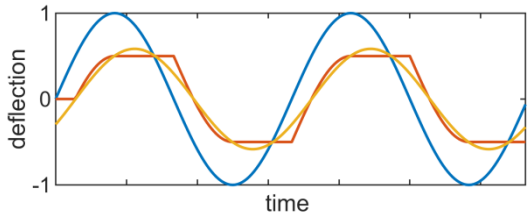

Figure 4 Effect of free play on the actuator; blue: commanded deflection, red: actual deflection, yellow: approximated actual deflection as sine curve

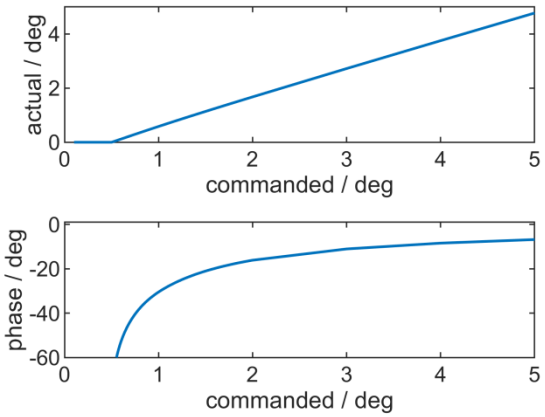

Figure 5 Describing function for free play nonlinearity

2.1 FREE PLAY

Free play is a very common nonlinearity in actuation systems but it should be kept as low as possible. It is known that free play is able to introduce limit cycle oscillations [9] reducing controller performance or even causing instabilities. Figure 4 shows the simulated response for free play nonlinearity. Therein the commanded sine signal features an amplitude of 1 deg and the actuator free play is set to 1 deg. The blue line shows the commanded deflection whereas the red line shows the actual deflection. The actual deflection starts to revert its direction when the commanded signal passes the 1 deg free play. Due to the free play nonlinearity a phase shift is introduced and also the amplitude is attenuated by half the free play. The yellow curve shows an approximation of the response with a single sine curve according to equation (1). However instead of directly applying this integral, the mathematical problem is reformulated and the coefficient a is approximated with a least squares solution.

Now the describing function for free play is derived. This function describes the fundamental harmonic response of a nonlinear function to sine excitation. In principle Figure 4 shows the result for one excitation amplitude. This is repeated for different excitation amplitudes with free play kept at 1 deg and results in the describing function, shown in Figure 5. The amplitude and phase shift of the approximated curves is plotted as a function of the commanded amplitude. If the commanded amplitude is increased, the ratio between free play and amplitude of the command signal decreases and the influence of the free play is reduced. Up to half the free play, the actuator is not following the command at all. After that, the actuator starts to move but the amplitude is attenuated and the phase shift is significant. With increasing amplitudes the attenuation is negligible and the phase shift is reduced as well. As one can see, free play results in a constant phase shift and constant amplitude attenuation.

2.2 DEFLECTION LIMIT

Apart from free play, the mechanical design of the actuator limits the maximum deflection. If the control law demands more deflection, the flap will run into mechanical limits and may collide with another part. As a safety measure, the deflection is restricted to a certain minimum and maximum value. This type of nonlinearity does not introduce a phase lag but decreases the amplitude if the commanded deflection is higher than the maximum deflection. Figure 6 shows the effect of deflection limit. It is notable that the approximated curve, yellow in the diagram, exceeds the maximum deflection amplitude. In this case the deflection limit is set to 10 deg, such that the nonlinear behavior will only take effect after the commanded signal exceeds 10 deg. Figure 7 shows the describing function for deflection limit. No phase loss occurs and the deflection reduces significantly if the commanded amplitude exceeds 10 deg. As seen in the previous figure, the approximated curve is able to exceed the 10 deg deflection limit.

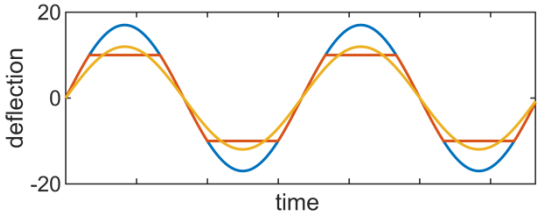

Figure 6 Effect of deflection limit on the actuator, blue: commanded deflection, red: actual deflection, yellow: approximated actual deflection as sine curve

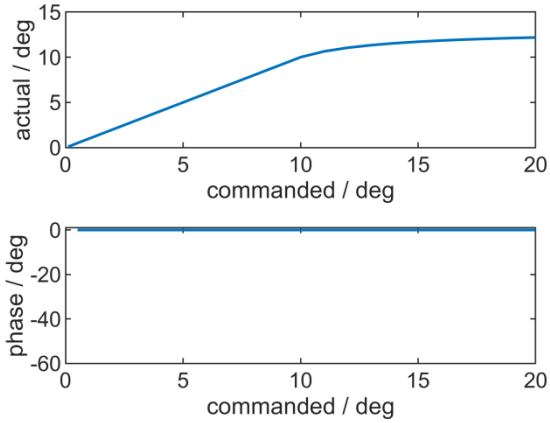

Figure 7 Describing function for deflection limit nonlinearity

2.3 RATE LIMIT

Another restriction of the servo motor is its limited power, which is defined as the product of torque and angular velocity, also denoted as angular rate. Since the servo cannot exceed a certain torque, the angular velocity is also limited. Additionally, other parts like bearings may limit the maximum velocity of the actuator. Note that actuator velocity may also be limited intentionally in order to reach a desired operating life time. This limitation is also called rate limit. In Figure 8, an example for rate limitation is given. Restricting the angular rate yields a triangular-like response, which becomes fully triangular when increasing the amplitude. This shape is caused by an upper and lower rate bound, which means that the first derivative is set constant when the rate limits are exceeded. Thus the actual deflection behaves linearly.

If the demand exceeds the rate limit, the actual deflection starts to lag behind and the maximum amplitude is not reached anymore. Figure 9 shows the describing function for rate nonlinearity. Because the rate limit nonlinearity also depends on frequency, the describing function is only valid for a certain frequency which is 15 Hz in this case. It is seen that no phase lag and no amplitude attenuation appears up to a commanded value of 10 deg. After that the amplitude is attenuated significantly and the actuator is phase shifted to the commanded signal.

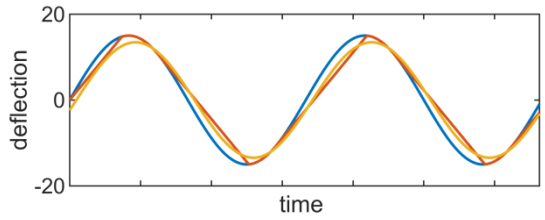

Figure 8 Effect of rate limit on the actuator, blue: commanded deflection, red: actual deflection, yellow: approximated actual deflection as sine curve

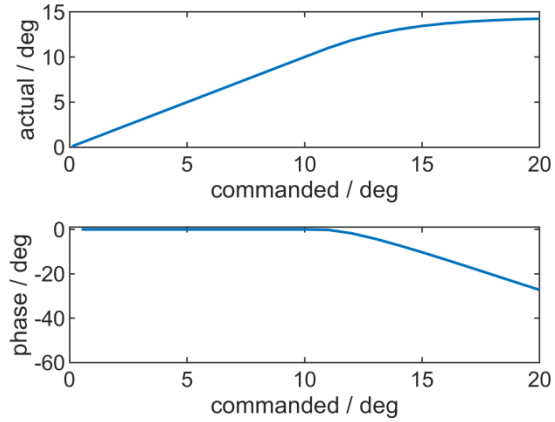

Figure 9 Describing function for rate limit nonlinearity

2.4 ACCELERATION LIMIT

As already mentioned, servo motors cannot apply more than the maximum torque, which limits the maximum acceleration of the control surface. Increasing the amplitude at constant harmonic frequency will also increase the acceleration, as increasing frequency with constant amplitude. This means that this nonlinearity is frequency dependent. If the demanded acceleration is too high, the actuator is not able to follow, which leads to amplitude attenuation and phase lag. The actuator is linear until the acceleration limit is reached, and afterwards, the effect of the nonlinearity increases with increasing amplitude. This type of nonlinearity is quite similar to rate limit, as seen in Figure 10.

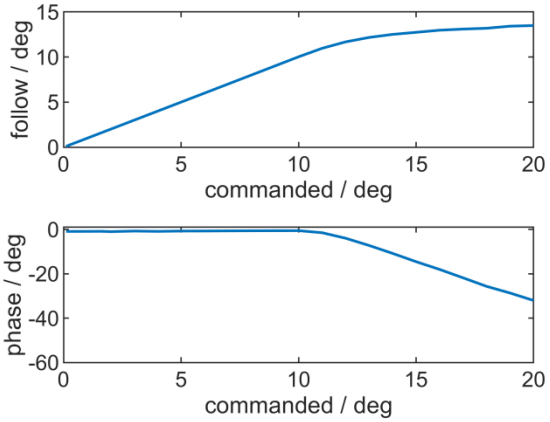

Figure 10 Describing function for acceleration limit nonlinearity

2.5 FURTHER NONLINEARITIES

Besides the described types of nonlinearities, also other nonlinearities like dead zone or friction are observed in actuation systems, which are not described in detail her since they have a minor impact on the considered control loop. Dead zone means that the system responds if a certain threshold is exceeded otherwise not. Friction is also a very common nonlinear behavior. Since the force in the actuation system is not modelled, no friction is seen. Another nonlinear behavior is jump resonance. In this phenomenon the response drastically increases or jumps for a small change. This typically happens if more than one response to a single excitation is possible, so that the system can jump between the possible solutions.

3 ACTUATION SYSTEM DESIGN

The actuation system of the considered flexible wing consists of a flap, a servo and a mechanical drive mechanism. The drive mechanism has a transmission ratio of 1:1 and is built with three rods, as indicated in Figure 11. The drive mechanism is necessary, since the servo cannot be placed at the hinge line of the flap due to the available space. The flap is mounted on the wing structure and is

driven by the mechanism, where each connection is a bearing which potentially introduces free play.

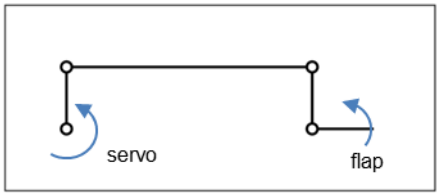

Figure 11 Sketch of the mechanics of the actuator

3.1 ACTUATOR REQUIREMENTS

In a first step of the design phase the servo motor is selected. This component dominates the dynamic behavior of the whole system. Ravenscroft [13] describes which performance properties for an actuation system of a full scale aircraft are important for flight control. Although those actuation systems are generally driven by hydraulic systems the requirements are comparable to the actuation system used in this test campaign. The stall load of the actuator is chosen, such that the actuator can hold its position even when the highest aerodynamic load is applied. The rate capability is important for pilot handling. In this work, no handling qualities are considered, so no minimum rate is defined but is can be assumed that the actuator bandwidth required for load alleviation is higher than the bandwidth for handling qualities. In contrast to flight control, the actuation system should be able to interact with the structural modes. This loads alleviation system increases the damping of the first structural mode, so the bandwidth of the chosen actuator should be double the eigenfrequency of the structural mode.

The minimum actuator requirement for the considered wing is a bandwidth up to 16 Hz and maximum deflection of 10 deg. Rate limits should be as high as possible and free play as small as possible. Maximum load is predicted to be negligible.

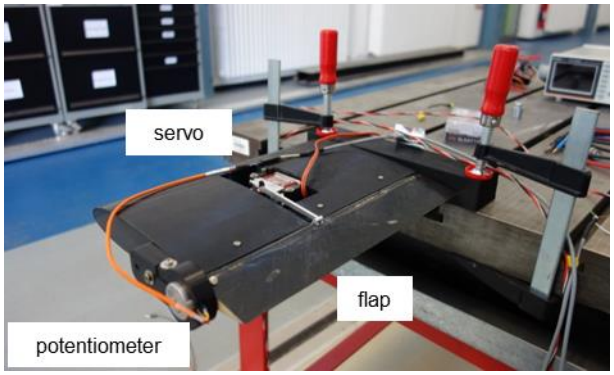

Figure 12 Test bed for early integration test. First design of the actuator is tested

3.2 TEST BED

The servo motor candidates were tested before the wing model was built. To enable this, a test rig was designed to emulate the boundary condition of the wing, shown in Figure 12. While the wing box consisted of a 3D printed mock-up, the flap in the test rig is the actual flap supposed to be integrated in the final wing. Also the mechanical drive mechanism between flap and servo represents the draft design for wing integration. The test already served as a first integration test to check for geometric constraints and mechanical limits to avoid collisions. In the end the mechanical design was slightly modified from the insights gained of this first integration test. For the experimental identification a potentiometer is attached on the extension of the control surface hinge line in order to measure the rotary deflection of the flap directly. The servo is embedded in the wing structure.

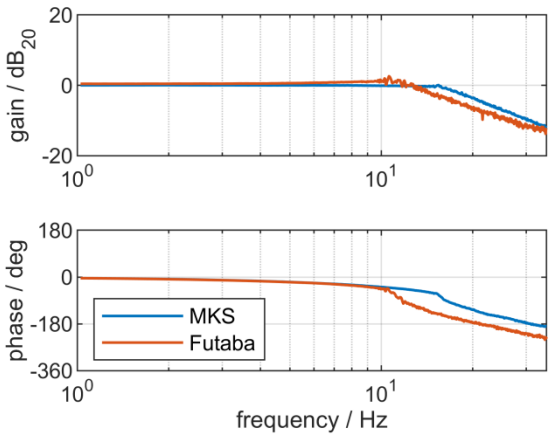

Figure 13 Comparison of the two servos in the test bed

Frequency responses of the Futaba BLS471SV, which was chosen by Regan [10], and a MKS BLH990 are compared in the test bed. The MKS motor was chosen as a second option due to promising specifications given by the manufacturer. Dead time, rate limit and frequency response is assessed and compared. Finally the MKS showed better dynamic behavior. A comparison of the two frequency responses can be seen in Figure 13. The bandwidth of the MKS servo is higher and the gain around the roll off frequency remains constant whereas the gain of the Futaba increases. Also linear phase response is seen up to approximately 10 Hz. More results on the dynamics of the MKS servo motor are presented in the next section.

3.3 ACTUATOR MODEL

It is preferable to have a detailed model of the servo motor, where all components are described with mathematical equations. But since the internal structure of the servo is unknown, especially the internal electronics and the position tracking controller, it is treated as black box model. Finally the actuation system is modelled as first order system extended by the nonlinear behavior described in

section 2. The structure of the model is shown in Figure 14. As input the commanded flap deflection is used. First the input is delayed by dead time. then the signal is fed through a first order system, such that the velocity is put out, then the signal is sequentially limited in acceleration and velocity. Finally the signal is integrated in time and free play as well as saturation is applied onto it. Finally the signal is derived again and put out as flap velocity. This input and output relation is necessary for the later integration into the whole model of the flexible wing.

Two sources of dead time may exist in this setup. First, the real time controller which is used for the loads alleviation runs with a sample rate of 1 kHz (i.e. outer control loop), and second, the internal position tracking controller of the servo (i.e. inner control loop), which is considered a black box. Dead time cannot be represented as a linear differential equation, thus it is often neglected in analysis but considered in the phase margin requirements within control design.

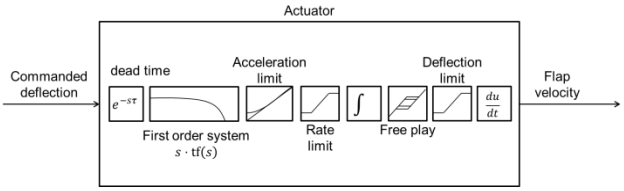

Figure 14 Structure of the nonlinear actuator model

4 EFFECT OF NONLINEARITIES ON CLOSED-LOOP PERFORMANCE

The expected nonlinear behavior is integrated into the simulation model of the flexible wing in order to investigate the impact of the nonlinearities on the controller performance. Pusch et. al [5] describes how the linear mathematical model is derived. The structural part of the model is derived finite element method and effectively reduced by truncation in modal space. The aerodynamic forces are modelled in the frequency domain using doublet lattice method and transformed into time domain using rational function approximation. All components are finally merged into a single integrated state space model. The block diagram for the described system is similar to Figure 2. Now the linear actuators are replaced by the nonlinear simulation model which is described in the previous section. All three actuators were assumed to be identical and have the same model properties at all time.

The simulation model enables gust excitation in terms of pitch excitation and gives the wing root bending moment response. Commanded flap deflection by the controller is significant for sine excitation frequency around 8 Hz close to the first structural mode. Pitch amplitude is set to 1 deg. As discussed earlier the nonlinear system will respond with multiple harmonics. Again the describing function method is used. Just the fundamental harmonic of the wing root bending moment to harmonic oscillation of the angle of attack is considered and the phase shift is given with respect to the pitch excitation. All nonlinearities are ignored in the beginning in order to compute a reference response of the system. Afterwards, each nonlinearity is studied individually by variation of the corresponding nonlinear parameter, while all other parameters remain constant. Proceeding this way helps to understand the impact of the different isolated nonlinearities on the controller performance. The results are always compared to the reference result of the linear case. Performance of the controller is defined as ratio of bending moment reduction. For evaluation purposes, the performance of the controller is defined as ratio of bending moment in open-loop and closed-loop configuration, as shown in equation (2).

$$P = \frac{M_i - M_{OL}}{M_{CL} - M_{OL}}, \tag{2}$$

where P is performance of the controller, M_{OL} is the root bending moment of the system without loads alleviation and $M_{CL}$is the root bending moment of the system with activated loads alleviation system. M_i is the current root bending moment for a specified nonlinear behavior. The reference loads reduction is 16.4 Nm and is represented in the denominator.

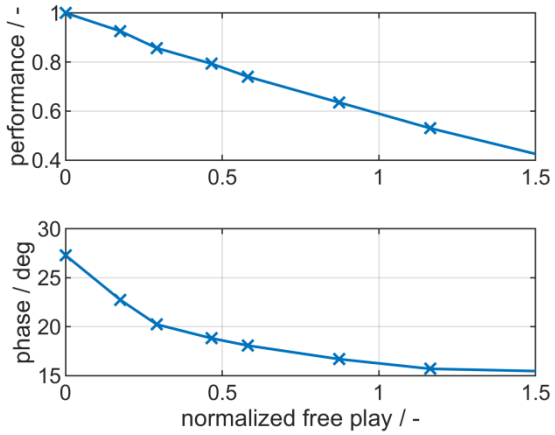

Figure 15 Varying free play and resulting performance loss of the controller

4.1 FREE PLAY

First, the free play parameter is investigated by variation from 0 to 4 deg. Although 1 deg is already a significant free play, the performance loss is only 16%. Increasing free play to 4 deg, controller performance loss is around 83%. Figure 15 depicts the described behavior. Free play is normalized with respect to the maximum reference deflection of 1.7 deg. The effect is rather small because the load alleviation controller is able to compensate the free play. If the flap deflection is too small, such that the flaps are not moving within the free play, the command signal is increased by the controller until the flap is effectively moving with adequate deflection. This results in loads reduction although the free play parameter is set to a higher value than the reference deflection, i.e. normal-

ized free play greater than 1. But this compensation also has limits if the free play is too large, because also the phase response drops with increasing free play.

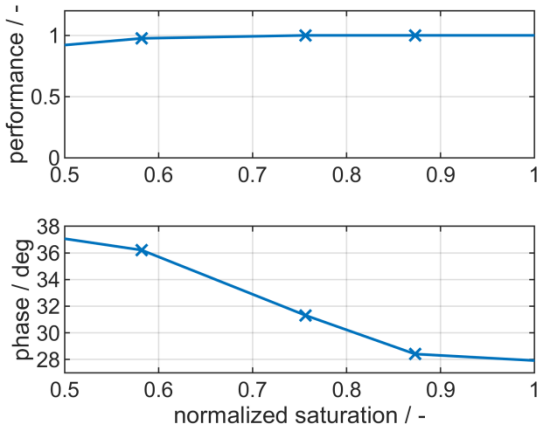

Figure 16 Varying deflection limit and resulting performance loss of the controller

4.2 DEFLECTION LIMIT

Subsequently, an artificial limit to the maximum displacement is used to study the impact of the saturation nonlinearity. The geometric constraint from wing design allows ±10 deg flap deflection. Under normal conditions, this limit is not reached. This means, that deflection commands are transmitted without any modification and the system remains in the linear regime. For this study, however, the saturation is reduced down to ±0.8 deg. It is normalized with respect to the reference command of 1.7 deg. This equals the flap command if no nonlinearities are active. The performance is hardly affected. Even if the deflection is limited to 60% of the reference flap command, the performance is still around 97% of the original moment reduction as it can be seen in Figure 16. Although the describing function from section 2.2 indicates no phase variation, the phase increases with increasing saturation.

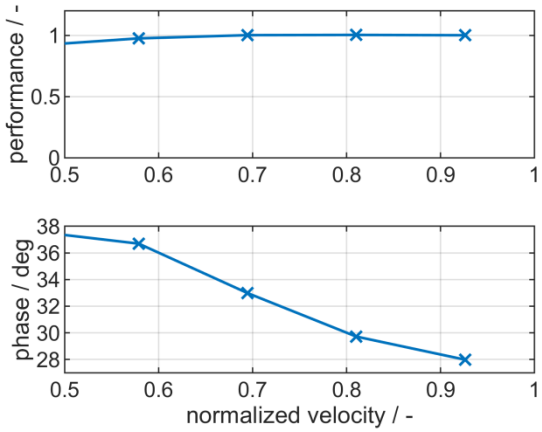

Figure 17 Varying rate limit and performance loss of the controller

4.3 RATE LIMIT

In a further study, the parameter of rate limit is investigated. Again, the rate limit is normalized with respect to the maximum reference velocity of 86.3 deg/s given by the controller in the linear case. Rate limits down to 60% of the reference response have no significant impact on the system. The performance is maintained at around 98% of the reference performance, see Figure 17. Also, the phase is increasing with increasing rate limit.

ACCELERATION LIMIT

Finally, the parameter of the torque limit is investigated. The given acceleration limit is normalized to the maximum reference acceleration of 4342 deg/s^2. If the acceleration limit is around 60% of the linear response, the performance of the controller drops to 50% of the linear performance. Thereby, the phase decreases with increasing acceleration limits. The rate limit and acceleration limit nonlinearities have a higher impact at higher frequencies. The velocity increases with increasing frequency but constant amplitude while the acceleration increases by the power of 2. Essentially, the impact of the acceleration limit is greater than the rate limit.

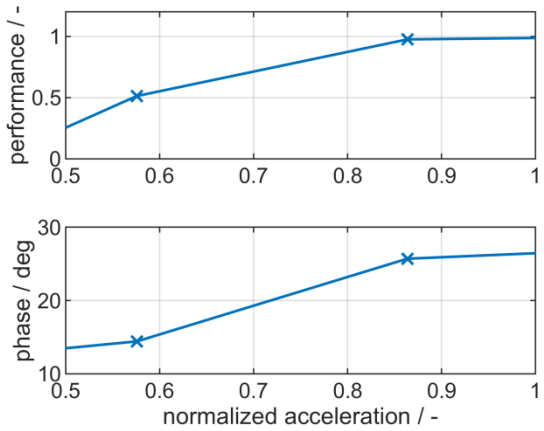

Figure 18 Varying acceleration limit and resulting performance loss of the controller

5 ACTUATOR IDENTIFICATION

Finally the parameters of the nonlinear system shown in Figure 14 needs to be identified. A common approach to non-parametric identification of a dynamic system is to excite the system with a known input signal and observe the output response. Depending on the intended usage of the identified model, typical excitation signals include step function, random or sine sweep. The sine sweep for example will focus the excitation energy on a narrow band sliding through the frequency range of interest, whereas with random excitation the excitation energy is spread over a broad frequency band. The sine sweep will thus lead to higher amplitudes and quasi-harmonic response which is preferable for nonlinear identification. After measuring the input signal $u(t)$ and output signal $y(t)$ the trans-

fer function $H(\omega)$ is computed as the ratio between output and input in frequency domain according to equation (3).

$$H(\omega) = \frac{Y(\omega)}{U(\omega)} \tag{3}$$

Note that this assumes linear dynamics meaning that the transfer function for nonlinear systems is actually not existent. In a first approach, however, the system is assumed to be linear and is identified according to this relation. The response at different amplitude levels will also reveal some information on the existence and type of nonlinearity. For example the linear phase loss is introduced by dead time. This parameter can be directly identified by determining the linear slope of the phase response.

The transfer behavior of the servo is identified at first in a non-parametric way using input-output transfer functions. Afterwards, dedicated test signals, following the methodology from Regan [10], are used to experimentally identify specific parameters of the different nonlinearities involved in the actuator model. The maximum achievable rate is identified from step function inputs and the free play parameter is quantified from sine excitation at a low frequency. The transfer functions measured at different amplitude levels reveal acceleration limit of the actuator. With the identified parameters a nonlinear Simulink model is established and can be included in the simulation model of this wind tunnel test.

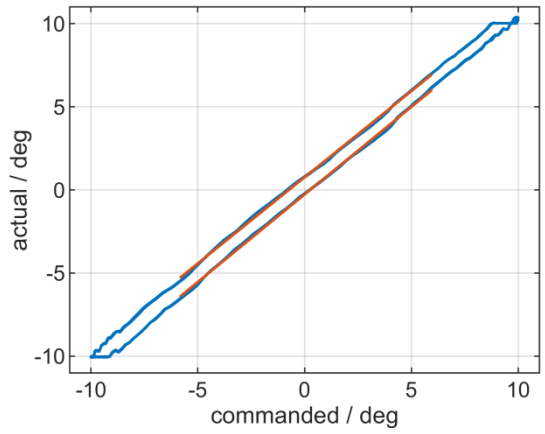

Figure 19 Blue line depicts the actual deflection over commanded deflection, hysteresis due to free play. The red line depicts is a linear regression for up and down movement. The offset equals the free play

5.1 FREE PLAY

A slow sine is used in order to estimate the free play. Figure 19 shows the results in terms of commanded flap signal to actual flap signal, measured by the potentiometer. A hysteresis is seen which is typical for free play. During the turning points the flap will not move until the free play is overcome. This deflection (i.e. the width of the hysteresis) equals the free play. The upward and downward path is identified as a linear function and the horizontal shift between the two is the free play.

5.2 RATE LIMIT

The rate limit of the actuator is tested using step functions of different step levels. The slope of the response is the rate limit. Figure 20 depicts the measured step responses. The blue line shows the response for a 7 deg step command signal and the yellow line represents the response of the actuator for a 57 deg step signal. The rate limit is estimated with linear regression. The purple line is fitted to the 57 deg step and the red line is fitted to the 7 deg step. The estimated slope for the response of the 7 deg step reveals a maximum velocity of 339 deg/s whereas the linear fit of the response of the 57 deg step shows a maximum velocity of 1129 deg/s. It seems that the maximum velocity increases with the step command. The reason for the different slopes is unknown but it is assumed that the torque limit might be responsible for this. There is simply not enough time for the actuator to reach the maximum velocity at smaller step commands. Also the unknown dynamics of the internal tracking controller might be a reason for this behavior.

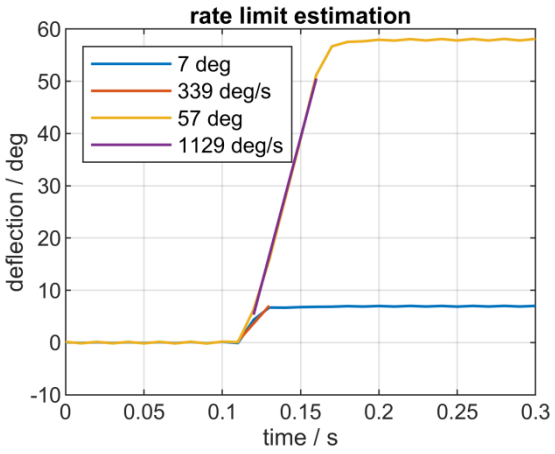

Figure 20 Estimation of the rate limit using a step function. Blue: 7 deg step response, yellow: 57 deg step response, red: identfied slope for 7 deg step, purple, identified slope for 57 deg step

5.3 ROLL OFF FREQUENCY AND DEAD TIME

In order to measure the dynamics for different amplitudes, sweep excitations are used. The results are shown in Figure 21 as deflection amplitude over frequency. From this, a linear model can be derived for each amplitude level. But it can be clearly seen (e.g. in the green curve in Figure 13) that the actuator runs into some kind of saturation at higher frequencies. Hence, a nonlinear model including rate and power limits is considered, where the actual saturation parameters need to be determined. The so called underlying linear model is identified from the low level run at 3 deg. As first order system the roll off frequency is feasible to describe the dynamics of the system.

Since the phase response is affected by dead time but not the amplitude response, only the amplitude response is used for roll off frequency identification. Also a linear phase loss is seen, indicating a dead time, which is identified from the linear slope of the phase response.

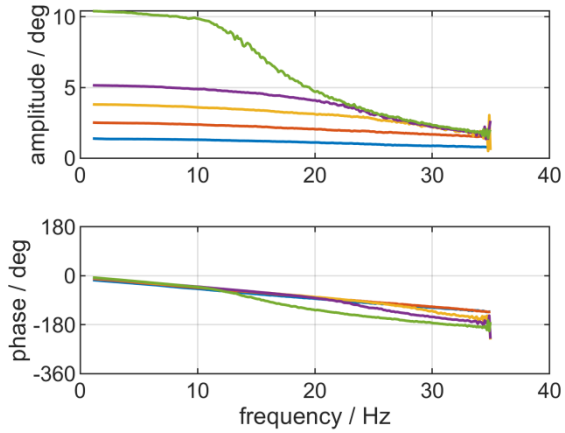

Figure 21 Frequency responses for different excitation level. Blue: 3 deg, red: 5 deg, yellow: 7.5 deg, purple: 10 deg, green: 20 deg

5.4 ACCELERATION LIMIT

The measured amplitude responses are integrated in frequency domain in order study the acceleration amplitude over frequency, see Figure 22. As one can see, the acceleration cannot exceed a certain value, which is the actual acceleration limit. This limitation depends on the actual torque limit of the actuator as well as on the inertia of the connected flap.

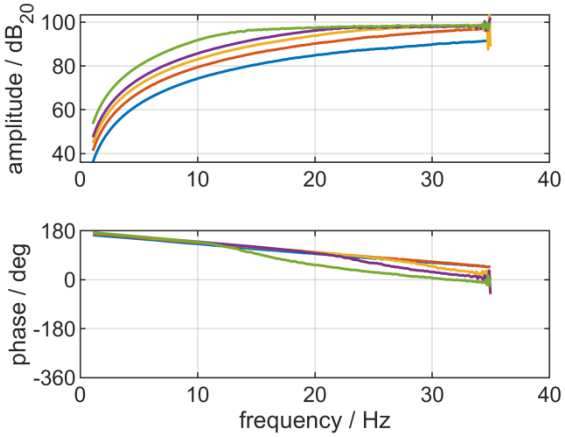

Figure 22 Acceleration response for different excitation level. Blue: 3 deg, red: 5 deg, yellow: 7.5 deg, purple: 10 deg, green: 20 deg

5.5 VALIDATION OF IDENTFIED PARAMETERS

The identified parameters, shown in Table 1, are used to build a nonlinear simulation model of the actuator. This model was tested in simulations and the results correspond well with the measured results, as can be seen in Figure 23. The match improves with higher amplitudes.

As already discussed, free play introduces a constant offset in phase and gain varying with amplitude. This effect is reduced for higher amplitudes as it can be seen in Figure 23. Another nonlinear effect is the amplitude dependent roll off, introduced by the acceleration limit.

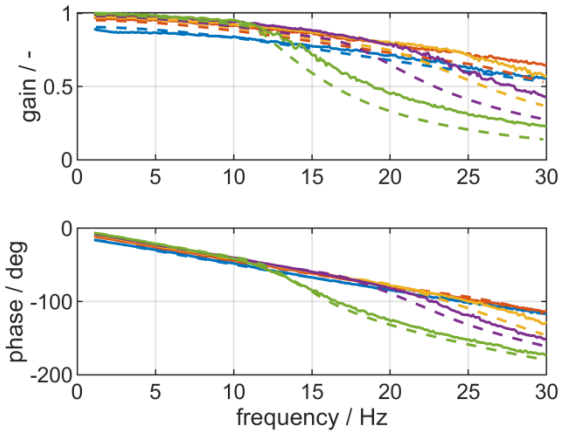

Figure 23 Comparison of measured and simulated actuator dynamics. Solid lines are measured and dashed lines simulated dynamics. Blue: 3 deg, red: 5 deg, yellow: 7.5 deg, purple: 10 deg, green: 20 deg

Table 1 identified parameters of the actuator

Parameter	Value
Roll off frequency	25 Hz
Dead time	4.3 ms
Free play	1 deg
Deflection limit	10 deg
Rate limit	1290 deg/s
Acceleration limit	79 540 deg/s²

6 CONCLUSION

A parametric nonlinear model of an electric flap actuator has been derived and implemented in Simulink. The corresponding model parameters were experimentally identified using a specially developed test bed

The nonlinear actuator model is integrated in an aero-servo-elastic simulation model including the unsteady aerodynamics and structural dynamics of the wing structure. The impact of the nonlinear parameters like free play, saturation, rate limit and torque limit on the performance of the load alleviation effectiveness have been investigated in simulations. Free play and power limit have the highest impact on the performance. Due to the nonlinearities the actual flap deflection is always smaller than it should be.

The simulations conducted with the linear equivalent model are therefore non-conservative because the root bending moment is higher when the nonlinear features of the actuator are taken into account. However, the controller designed for the linear system will partially compensate this and increase the command, such that the measured load is decreased again. But because of the phase response of the free play, the controller is not always able to fully compensate the nonlinear effect. Finally the parameters for the actuation system used for the mentioned survey are identified in a test bed.

A framework has been built which allows the investigation of different nonlinearities on the performance of a controller. Due to computation time reasons the controller should be designed using a linearized actuator model. But the impact of nonlinearities on the performance of the final controller design can be assessed with the nonlinear actuator model.

ACKNOLEDGEMENTS

The authors would like to thank Mr. Tobias Meier for his valuable support in building up the testbed for actuator identification. This work was commonly conducted by the DLR-Institute of Aeroelasticity and DLR-Institute of System Dynamics and Control within the DLR-internal Aeronautical Research Project “KonTeKst”.

REFERENCES

1. Dillinger, J., et al., *Design and optimization of an aeroservoelastic wind tunnel model*, in *IFASD 2019 - International Forum on Aeroelasticity and Structural Dynamics*. 2019: Savannah, GA (USA).
2. Krüger, W.R., et al., *Design and wind tunnel test of an actively controlled flexible wing*, in *International Forum on Aeroelasticity and Structural Dynamics*. 2019: Savannah, GA (USA).
3. Ossmann, D. and M. Pusch, *Fault Tolerant Control of an Experimental Flexible Wing.* 2019. **6**(7): p. 76.
4. Fung, Y.-c., *An introduction to the theory of aeroelasticity*. 1955: Wiley.
5. Pusch, M., et al., *Aeroelastic Modeling and Control of an Experimental Flexible Wing*, in *AIAA SciTech Forum*. 2019: San Diego, USA.
6. Taylor, R., R.W. Pratt, and B.D.J. Caldwell, *The application of actuator performance limits to aeroservoelastic compensation.* Transactions of the Institute of Measurement Control, 1999. **21**(2-3): p. 106-112.
7. Fielding, C. and P.K. Flux, *Non-linearities in flight control systems.* Aeronautical Journal, 2003. **107**(1077): p. 673-686.
8. Stirling, R. and D. Cowling. *Implementation of Comprehensive actuation system models in aeroservoelastic analysis*. in *European Forum on Aeroservoelasticity and Structural Dynamics, Aachen, Germany, report no. SDL*. 1989.
9. Banavara, N.K. and J.R. Newsom, *Framework for Aeroservoelastic Analyses Involving Nonlinear Actuators.* Journal of Aircraft, 2012. **49**(3): p. 774-780.
10. Regan, C. *mAEWing2: Conceptual design and system test*. in *AIAA Atmospheric Flight Mechanics Conference, 2017*. 2017.
11. Theis, J., H. Pfifer, and P.J. Seiler. *Robust control design for active flutter suppression*. in *AIAA Atmospheric Flight Mechanics Conference*. 2016.
12. Pusch, M., D. Ossmann, and T. Luspay, *Structured Control Design for a Highly Flexible Flutter Demonstrator.* 2019.
13. Pratt, R.W., *Flight control systems*. 2000: American Institute of Aeronautics and Astronautics.